

Low-noise $\text{YBa}_2\text{Cu}_3\text{O}_{7-\delta}$ direct-current superconducting quantum interference device magnetometer with direct signal injection

L. P. Lee, J. Longo, V. Vinetskiy, and R. Cantor
Conductus, Inc., Sunnyvale, California 94086

(Received 21 September 1994; accepted for publication 3 January 1995)

We have fabricated several low-noise direct-current superconducting quantum interference device (SQUID) magnetometers from single layers of $\text{YBa}_2\text{Cu}_3\text{O}_{7-\delta}$ on $10\text{ mm} \times 10\text{ mm}$ bicrystal substrates. The magnetometer design consists of a single-turn pickup loop that is directly coupled to the SQUID inductance. At 77 K, these magnetometers exhibit large voltage modulation with applied flux of over $40\text{ }\mu\text{V}$. The minimum flux noise, measured at 77 K using conventional flux-locked loop electronics with bias current reversal, is $3.5 \times 10^{-6}\text{ }\Phi_0/\sqrt{\text{Hz}}$ above 10 kHz and $6.5 \times 10^{-6}\text{ }\Phi_0/\sqrt{\text{Hz}}$ at 1 Hz. The field-to-flux conversion efficiency is measured to be $10\text{ nT}/\Phi_0$, resulting in a white magnetic field noise of $35\text{ fT}/\sqrt{\text{Hz}}$ above 10 kHz, increasing to $65\text{ fT}/\sqrt{\text{Hz}}$ at 1 Hz. © 1995 American Institute of Physics.

During the past few years, there has been considerable progress in the development of thin-film high- T_c superconducting quantum interference devices (SQUIDs) with low magnetic flux noise at 77 K.¹ To ensure low noise operation, these bare SQUIDs are necessarily low inductance devices; typical values of the SQUID inductance L are about 100 pH or less. Consequently, a bare SQUID generally has a low effective flux capture area A_s , resulting in a magnetic field resolution that is insufficient for many applications. For these applications, it is advantageous to use a separate signal or pickup coil that can have a much larger flux capture area. The pickup coil is connected to a multiturn spiral input coil that can be transformer coupled to the SQUID inductance. For best coupling, this is ideally done by patterning the SQUID inductance in the shape of a washer with the input coil integrated on top.² Alternatively, the flux transformer and SQUID may be fabricated on separate chips and then pressed together in a “flip-chip” configuration.^{3–5} In principle, the design of such flux transformers is straightforward, but the fabrication of these multilayer structures using high- T_c superconductors is not. A further complication is that, even though high- T_c flux transformers with excellent electrical transport properties have been fabricated, substantial low-frequency $1/f$ noise is observed for frequencies f below 1 kHz when coupled to the SQUID.^{6,7} For these reasons, transformer-coupled high- T_c SQUIDs (HTSQUIDs) remain unattractive for low frequency applications. A different approach is to take advantage of the flux focusing effect of a large superconducting washer.⁸ In this way, the effective area of the SQUID may be enhanced without increasing the SQUID inductance. Using this approach, Zhang *et al.*⁹ report a magnetic field noise of $170\text{ fT}/\sqrt{\text{Hz}}$ for frequencies down to 1 Hz for a large washer rf SQUID operating at 77 K. Another approach is to couple the signal from the pickup loop to the SQUID by direct injection,^{5,10–12} a configuration in which the SQUID inductance is connected in parallel with the pickup loop. Although the inductance mismatch is substantial, reasonable coupling, and a significant enhancement of the effective area can be achieved. Koelle *et al.*¹² report a field noise of $93\text{ fT}/\sqrt{\text{Hz}}$ at 1 Hz for a direct-coupled dc

SQUID magnetometer at 77 K. A significant advantage of these two latter approaches is that the complete device can be fabricated from a single layer of high- T_c superconductor. In this letter we describe the design of a direct-coupled dc SQUID magnetometer and report recent results obtained for several of these devices.

For a magnetometer, the relevant figure of merit for most applications is the rms magnetic flux density noise $S_B^{1/2}(f) = S_\Phi^{1/2}(f)/A_{\text{eff}}$. Here, $S_\Phi^{1/2}(f)$ is the rms flux noise and A_{eff} is the effective flux capture area of the magnetometer, which may also be expressed in terms of the field-to-flux conversion efficiency $B_\Phi = \Phi_0/A_{\text{eff}}$. Thus, the magnetic field noise of a directly coupled magnetometer can be optimized by minimizing the flux noise and maximizing the effective area.

The magnetic flux noise $S_\Phi^{1/2}(f) = S_V^{1/2}(f)/(\partial V/\partial\Phi)$, where $S_V^{1/2}(f)$ is the rms voltage noise across the SQUID and $\partial V/\partial\Phi$ is the flux-to-voltage transfer function. In the absence of excess noise due to poor film quality, junction parameter fluctuations or resonances, one may model the voltage noise as arising from two nearly uncorrelated noise currents in the SQUID, one circulating around the SQUID loop and the other through the SQUID.¹³ Then, neglecting the noise of the room temperature preamplifier, the voltage noise may be written as¹³ $S_V(f) = (\partial V/\partial\Phi)^2 L^2 4k_B T / (2R) + 4k_B T R_{\text{dyn}}$, where R is the junction resistance and $R_{\text{dyn}} = \partial V/\partial I$ is the dynamic resistance of the SQUID. The flux noise becomes¹³

$$S_\Phi(f) = L^2 4k_B T / (2R) + (\partial V/\partial\Phi)^{-2} k_B T R_{\text{dyn}}. \quad (1)$$

For operation at a given temperature T , the SQUID must therefore have a low inductance and high flux-to-voltage transfer coefficient.

According to conventional SQUID analysis,¹⁴ $\partial V/\partial\Phi \propto I_c R / (1 + \beta)$, where $\beta = 2LI_c/\Phi_0$ and I_c is the critical current per junction. For dc SQUIDs operating at 77 K, however, much lower transfer coefficients are observed than the conventional analysis predicts. Enpuku *et al.*¹⁵ have recently shown that this discrepancy is due to thermal noise. They show that the total integrated thermal noise flux $\delta\Phi_n = \sqrt{k_B T L}$ of a SQUID operating at 77 K can be a significant

fraction of Φ_0 and cause a significant reduction of the maximum peak-to-peak voltage modulation of the SQUID ΔV . According to their simulations,

$$\Delta V = \frac{4}{\pi} \frac{I_c R}{1 + \beta} \left(1 - 3.57 \frac{\sqrt{k_B T L}}{\Phi_0} \right). \quad (2)$$

Assuming a sinusoidal voltage modulation with applied flux, $\partial V / \partial \Phi = \pi \Delta V$; thus, any degradation of the voltage modulation leads to a reduction of $\partial V / \partial \Phi$ and an increase of the rms magnetic flux noise $S_\Phi^{1/2}(f)$. For operation at 77 K, Eq. (2) implies the need to use the lowest possible SQUID inductance and junctions exhibiting a large $I_c R$ product. There are two limitations, however: coupling to the SQUID with reasonable efficiency becomes increasingly difficult as the SQUID inductance decreases, and according to conventional SQUID theory,¹⁴ the optimal energy resolution $\epsilon = S_\Phi / 2L$ occurs for $\beta \approx 1$. This means the critical current I_c must increase proportionally to offset any decrease in L . The latter is not necessarily a limitation since a high $I_c R$ product is desired, but a large critical current may be accompanied by fluctuations which can degrade the anticipated SQUID voltage modulation¹⁶ and in turn the magnetometer performance. For this reason, it may be advantageous to choose a low design value for the critical current, provided a high $I_c R$ product can be maintained. This requires low critical current, high resistance Josephson junctions. Here the limitation is that the Josephson coupling energy must be larger than the thermal energy. It has been shown¹⁷ that a factor of 5 times larger should be sufficient, which gives a minimum critical current of 16 μA at 77 K. Using the condition $\beta \approx 1$, the corresponding maximum SQUID inductance is about 65 pH.

The effective flux capture area of the magnetometer is given by $A_{\text{eff}} = A_s + k(A_p/L_p)L \approx k(A_p/L_p)L$, where A_s is the effective area of the SQUID loop, A_p is the effective area of the pickup loop with inductance L_p , and k is a constant which describes the coupling efficiency. Thus, for a given SQUID inductance L , it is necessary to maximize the ratio A_p/L_p and the coupling constant k . The coupling constant is optimized by maximizing the fraction of the SQUID inductance seen by the injected signal current. For the magnetometers described here, the SQUID is formed from a 65 μm long, 20 μm wide strip of $\text{YBa}_2\text{Cu}_3\text{O}_{7-\delta}$ (YBCO) with a 55 μm long, 4 μm wide slit along its length. The 10 μm long, 3 μm wide grain boundary junctions are located at the outer end of the slit, along with the two, 5 μm wide injection leads for the signal current in the pickup loop. The SQUID inductance may be written as the sum of two parts, $L = L_{\text{sl}} + L_j$, where L_{sl} is the slit inductance and L_j is the parasitic inductance associated with the junctions. To calculate these inductances we use standard inductance formulas for coplanar lines.¹⁸ We calculate $L_{\text{sl}} = 42$ pH and $L_j = 13$ pH, which include kinetic inductance¹⁹ contributions of 6 and 4 pH, respectively. Then, the total inductance $L = 55$ pH, and the coupling constant is approximately given by $k \approx L_{\text{sl}}/L = 0.76$. From measurements on similar SQUIDS, we have determined the quantity kL directly by cutting the pickup loop and injecting an external current into the SQUID. The measurements agree with the inductance calculations to better than 5%.

For a square loop with outer side length a and inner side length d , it can be shown that the ratio A_p/L_p gradually approaches a maximum in the limit $(a-d)/2 \gg d$. In this limit,² $A_p = ad$ and $L_p = 1.25 \mu_0 d$, so that $A_p/L_p = a/1.25 \mu_0 = 0.637a[\text{mm}]\text{mm}^2/\text{nH}$. Using the expression for the coupling constant k given above, the effective area of the magnetometer $A_{\text{eff}} \approx 0.637a[\text{mm}]L_{\text{sl}}[\text{nH}]\text{mm}^2$. The magnetometers described below are fabricated on 10×10 mm^2 substrates. We therefore use $a = 9.3$ mm, with $d = 3$ mm in order to satisfy the condition $(a-d)/2 \gg d$. For these parameter values, $A_p \approx 28$ mm^2 and $L_p \approx 4.7$ nH. Using $L_{\text{sl}} = 0.042$ nH, we calculate $A_{\text{eff}} \approx 0.25$ mm^2 . We have determined A_{eff} directly by measuring the magnetometer response in a uniform magnetic field provided by a Helmholtz coil. We find that the field-to-flux conversion efficiency $B_\Phi = 10$ nT/ Φ_0 , which yields $A_{\text{eff}} \approx 0.21$ mm^2 , in reasonable agreement with the calculation. The small difference may be accounted for by a missing strip of pickup loop occupied by a row of four 1×1 mm^2 contact pads which is estimated to reduce A_p , and therefore A_{eff} , by 20%.

The magnetometers are fabricated from 150 to 300 nm thick c -axis oriented $\text{YBa}_2\text{Cu}_3\text{O}_{7-\delta}$ (YBCO) films on 10×10 mm^2 SrTiO_3 bicrystal substrates with a 24° misorientation angle. The YBCO films are patterned by ion milling through a photoresist mask. The contact pads are covered by a gold layer which is ion beam deposited through a photoresist lift-off stencil.

For the dc and noise measurements, the magnetometers are mounted onto fiberglass-epoxy printed circuit (PC) boards. Electrical connections to the chip are provided by gold wire bonds, while the contacts to the PC board are made using spring-loaded contact pins. The electrical measurements are carried out in a rf shielded room. The SQUID magnetometer packages are immersed in liquid nitrogen in a Dewar surrounded by at least three μ -metal shields. For the noise measurements, an additional cooled μ -metal shield is mounted around the magnetometers. The SQUID is operated in a flux-locked loop using 500 kHz flux modulation and either static or ac current bias.²⁰ The frequency of the ac current bias is generally 2 kHz or higher.

We have fabricated grain boundary junctions with resistances as high as 20 Ω per junction and $I_c R$ products typically of the order of 100 μV . The I - V characteristics of a typical magnetometer for applied flux $\Phi_a = 0$ and $\Phi_0/2$ are shown in Fig. 1. For this device, we calculate $I_c = 9.5$ μA by fitting the I - V characteristic for $\Phi_a = 0$ to the Ambegaokar-Halperin²¹ model using the measured asymptotic resistance $R = 13.8$ Ω . Thus, for this device $\beta \approx 0.5$. Owing to the high junction resistance, this SQUID is observed to be hysteretic at 4.2 K. The maximum voltage modulation $\Delta V = 42$ μV is observed for bias current $I_b = 11$ μA . According to Eq. (2), the predicted voltage modulation for this device is 65 μV . We believe the discrepancy between the predicted and experimentally measured values is primarily due to the broad step in the I - V characteristic for $\Phi_a = \Phi_0/2$ around 80 μV . This current step is likely a signature of a microwave resonance at the frequency $f_r = (80 \times 10^{-6})/\Phi_0 = 39$ GHz in the pair of coplanar lines which form the

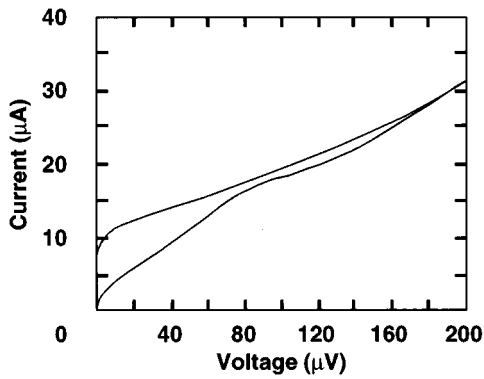


FIG. 1. Current–voltage characteristics measured at 77 K for an applied flux corresponding to 0 (upper curve) and $\Phi_0/2$ (lower curve).

SQUID body. Since the phase velocity $v=c\sqrt{2/(\epsilon_r+1)}$ is independent of the geometry, the most likely resonance corresponds to a quarter wavelength along the total length $l=60\ \mu\text{m}$ from the end of the slit to the Josephson junctions where there is a large impedance change due to the junction resistance. The corresponding resonant frequency $f_r=(c/4l)\sqrt{2/(\epsilon_r+1)}$. We have determined the dielectric constant of the SrTiO₃ bicrystal substrate at 77 K using a confocal resonator and find $\epsilon_r=1930$. Using this value, we calculate $f_r=40\ \text{GHz}$, in good agreement with the experimentally observed resonant frequency. We note further that no such resonances are observed for similar SQUIDs fabricated on YSZ substrates, and the maximum voltage modulation observed for these devices is only about 15% lower than predicted using Eq. (2). The dielectric constant of YSZ is significantly lower, and the coplanar line resonance therefore occurs at a much higher frequency.

The best measured magnetic field and flux noise is shown in Fig. 2. We have measured comparable noise on several magnetometers of this type. The field noise measured using dc current bias is $28\ \text{fT}/\sqrt{\text{Hz}}$ above 10 kHz and has a $1/f$ dependence below 100 Hz. The low frequency noise is improved considerably using bias current reversal²⁰ at 16 kHz,

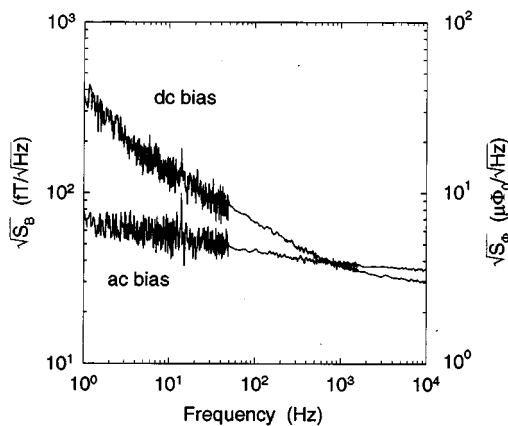


FIG. 2. Measured rms magnetic field noise, $S_B^{1/2}(f)$, and rms flux noise, $S_\Phi^{1/2}(f)$, at 77 K vs frequency for conventional flux-locked loop operation with dc current bias (upper curve) and with ac current bias at 16 kHz (lower curve).

although some frequency-dependent noise remains. The white field noise with ac bias above 10 kHz is $35\ \text{fT}/\sqrt{\text{Hz}}$ and increases slowly for lower frequencies, becoming $65\ \text{fT}/\sqrt{\text{Hz}}$ at 1 Hz. The white flux noise using dc bias is $2.8 \times 10^{-6}\ \Phi_0/\sqrt{\text{Hz}}$, from which the energy resolution $\epsilon=S_\Phi(f)/2L=3 \times 10^{-31}\ \text{J/Hz}$. This is about a factor of 8 times higher than predicted according to the theoretical result¹ $\epsilon=9k_B T L/R$. The discrepancy may in part be caused by the observed SQUID microwave resonance²² owing to the large substrate dielectric constant. The origin of the excess noise at low frequencies is not clear, but may be due to environmental effects, flux motion in the YBCO film, or the presence of thermally activated phase slippage.²³

In summary, we have designed and fabricated several low-noise, single-layer YBCO SQUID magnetometers on SrTiO₃ bicrystal substrates. The Josephson junctions have low critical current and high resistance such that the $I_c R$ produce is of the order of $100\ \mu\text{V}$. These devices exhibit large voltage modulation with applied flux, leading to very low flux noise. The magnetic field noise is believed to be the lowest reported to date for a single-layer dc SQUID magnetometer on a $1\ \text{cm}^2$ substrate operating at 77 K.

The authors thank John Clarke, Dieter Koelle, and Keiji Enpuku for helpful discussions.

¹See, for example, J. Clarke, in *The New Superconducting Electronics*, edited by H. Weinstock and R. W. Ralston (Kluwer, Dordrecht, 1993), pp. 123–180, and references therein.

²J. M. Jaycox and M. B. Ketchen, IEEE Trans. Magn. **MAG-17**, 400 (1981).

³A. H. Miklich, J. J. Kingston, F. C. Wellstood, and J. Clarke, Appl. Phys. Lett. **59**, 988 (1991).

⁴D. Koelle, A. H. Miklich, F. Ludwig, E. Dansker, D. T. Nemeth, J. Clarke, W. Ruby, and K. Char, Appl. Phys. Lett. **63**, 3630 (1993).

⁵A. H. Miklich, D. Koelle, E. Dantsker, D. T. Nemeth, J. J. Kingston, R. F. Kromann, and J. Clarke, IEEE Trans. Appl. Supercond. **3**, 2434 (1993).

⁶M. Ferrari, J. J. Kingston, F. C. Wellstood, and J. Clarke, Appl. Phys. Lett. **58**, 1106 (1991).

⁷F. Ludwig, E. Dantsker, D. T. Nemeth, D. Koelle, A. H. Miklich, and J. Clarke, Supercond. Sci. Technol. **7**, 273 (1994).

⁸M. B. Ketchen, W. J. Gallagher, A. H. Kleinsasser, S. Murphy, and J. R. Clem, in *SQUID '85 Superconducting Quantum Interference Devices and their Applications*, edited by H. Hahlbohm and H. Lübbig (Springer, Berlin, 1985), pp. 865–871.

⁹Y. Zhang, M. Mück, K. Hermann, J. Schubert, W. Zander, A. I. Braginski, and C. Heiden, IEEE Trans. Appl. Supercond. **3**, 2465 (1993).

¹⁰M. Matsuda, Y. Murayama, S. Kiryu, N. Kasai, S. Kashiwaya, M. Koyanagi, and T. Endo, IEEE Trans. Magn. **MAG-27**, 3043 (1991).

¹¹S. Knappe, D. Drung, T. Schurig, H. Koch, M. Klinger, and J. Hinken, Cryogenics **132**, 881 (1992).

¹²D. Koelle, A. H. Miklich, E. Dantsker, D. T. Nemeth, and J. Clarke, Appl. Phys. Lett. **63**, 2271 (1993).

¹³T. Ryhänen, H. Seppä, R. Limoniemi, and J. Knuutila, J. Low Temp. Phys. **76**, 287 (1989).

¹⁴C. D. Tesche and J. Clarke, J. Low Temp. Phys. **29**, 301 (1977).

¹⁵K. Enpuku, Y. Shimomura, and T. Kisu, J. Appl. Phys. **73**, 7929 (1993).

¹⁶K. Enpuku, Jpn. J. Appl. Phys. **32**, L1407 (1993).

¹⁷J. Clarke and R. Koch, Science **242**, 217 (1988).

¹⁸K. C. Gupta, R. Garg, and I. J. Bahl, *Microstrip Lines and Slotlines* (Artech House, Dedham, MA, 1979), pp. 263–265.

¹⁹R. Meservey and P. M. Tedrow, J. Appl. Phys. **40**, 2028 (1969).

²⁰M. B. Simmonds and R. P. Giffard, U.S. Patent No. 4,389,612 (21 June 1983); R. H. Koch, J. Clarke, W. M. Goubau, J. M. Martinis, C. M. Pegrum, and D. J. Van Harlingen, J. Low Temp. Phys. **51**, 207 (1983).

²¹V. Ambegaokar and B. I. Halperin, Phys. Rev. Lett. **22**, 1364 (1969).

²²T. Ryänen, H. Seppä, and R. Cantor, J. Appl. Phys. **71**, 6150 (1992).

²³R. Gross, P. Chaudhari, D. Dimos, A. Gupta, and G. Koren, Phys. Rev. Lett. **64**, 228 (1990).